

# Boundaries on Neutrino Mass from Supernovae Neutronization Burst by Liquid Argon Experiments

F. Rossi-Torres,<sup>\*</sup> M. M. Guzzo,<sup>†</sup> and E. Kemp<sup>‡</sup>

*Instituto de Física Gleb Wataghin, Universidade Estadual de Campinas - UNICAMP,  
Rua Sérgio Buarque de Holanda, 777, 13083-859, Campinas-SP, Brazil*

This work presents an upper bound on the neutrino mass using the emission of  $\nu_e$  from the neutronization burst of a core collapsing supernova at 10 kpc of distance and a progenitor star of  $15 M_\odot$ . The calculations were done considering a 34 kton Liquid Argon Time Projection Chamber similar to the Far Detector proposal of the Long Baseline Neutrino Experiment (LBNE). We have performed a Monte Carlo simulation for the number of events integrated in 5 ms bins. Our results are  $m_\nu < 2.71$  eV and  $0.18$  eV  $< m_\nu < 1.70$  eV, at 95% C.L, assuming normal hierarchy and inverted hierarchy, respectively. We have analysed different configurations for the detector performance resulting in neutrino mass bound of  $\mathcal{O}(1)$  eV.

## I. INTRODUCTION

From the current experimental evidence of neutrino oscillations [1, 2], we know that neutrinos are massive particles, and each neutrino flavor eigenstate  $|\nu_\beta\rangle$  ( $\beta = e, \mu, \tau$ ) is a coherent superposition of mass eigenstates  $|\nu_i\rangle$  ( $i = 1, 2, 3$ ), connected by the PMNS mixing matrix  $U_{\beta i}$ , through the relation  $|\nu_\beta\rangle = \sum_i U_{\beta i} |\nu_i\rangle$ . However, oscillation experiments are sensitive only to the mass squared differences ( $\Delta m_{ij}^2 = m_i^2 - m_j^2$ ;  $i, j = 1, 2, 3$ ) and not on the absolute value of each mass eigenstate which is one of the most challenging measurement in particle physics. Furthermore, one must be careful about the interpretation of experiments on neutrino masses since different techniques result in different observables. For instance, neutrino-less double beta decay experiments search for Majorana neutrinos with mass  $m_{ee}^2 = |\sum_i U_{ei}^2 m_i|^2$  and single- $\beta$  decay experiments observe features driven by massive neutrinos with  $m_e^2 = \sum_i |U_{ei}^2|^2 m_i^2$  not dependent on Majorana phases. Since  $m_e > m_{ee}$  measurements which are not exclusively sensitive to Majorana neutrinos can be safely taken as conservative ones [3].

If we can measure the mass of any neutrino flavor  $\nu_\beta$  the masses of  $\nu_i$  can be obtained from the boundaries of the mixing matrix and other  $\Delta m_{ij}^2$  obtained from different oscillation experiments.

The strongest experimental limit in the neutrino mass, as quoted in the Particle Data Group (PDG) [4], was obtained by the Troitsk experiment on tritium single- $\beta$  decay:  $m_e < 2.05$  eV at 95% confidence level (C.L) [5]. This kind of experiment measures the modification of the  $\beta$  spectrum near its endpoint caused by the neutrino mass. The KATRIN experiment [6] will improve the technique and plan to set a stronger limit by enhancing the sensitivity at least in one order of magnitude.

Neutrinos emitted from stellar collapse, for example type II supernovae, can give a valuable contribution to the determination of the mass of neutrinos, as idealized by Zatsepin [7]. Using neutrino data [8–10] from the SN1987A, which exploded in the Large Magellanic cloud ( $\sim 50$  kpc), and the likelihood of detection analysis proposed in [11], an upper bound of 5.8 eV at 95% C.L [12] was obtained. With a different likelihood approach and astrophysical parametrization of the neutrino emission, Lamb & Loredó [13] reached a 5.7 eV at 95% C.L for the neutrino mass limit.

There are good perspectives to explore the sub-eV region in the future experimental scenario for detection of galactic supernovae [12, 14–17]. Other mass limits obtained from the supernovae can be seen in the table presented in Ref. [18].

The perspective to detect  $\nu_e$  from a supernova, but in a liquid scintillator detector, was recently considered in [19, 20]. Water Cherenkov detectors with Gadolinium could also improve the number of  $\nu_e$  events according to [21]. In the present work, we aim to discuss bounds on neutrino masses from supernovae motivated by the Zatsepin's idea. We are going to consider electronic neutrinos ( $\nu_e$ ) emitted from the neutronization burst of a galactic supernova at a distance of 10 kpc and  $15 M_\odot$  and detected by a Liquid Argon Time Projection Chamber (LArTPC).

The paper is organized as follow: Sec. II presents the main assumptions about electronic neutrino production and its propagation; Sec. III presents the basic features about the neutrino detection in the LArTPC; Sec. IV presents

---

<sup>\*</sup>Electronic address: ftorres@ifi.unicamp.br

<sup>†</sup>Electronic address: guzzo@ifi.unicamp.br

<sup>‡</sup>Electronic address: kemp@ifi.unicamp.br

the main assumptions about our event generated Monte Carlo simulation and Sec. V presents the boundaries on the neutrino mass. Sec. VI and Sec. VII present the discussion about our results and our main conclusions, respectively.

## II. NEUTRINOS FROM SUPERNOVAE

As the shock evolves against the infalling dense matter of the outer core of the star, some of its energy is lost by the photodissociation of nuclei into protons and neutrons. At this moment, there is an abundant production of electronic neutrinos ( $\nu_e$ ) via  $p + e^- \rightarrow n + \nu_e$ . These electronic neutrinos accumulate in a very dense and opaque environment behind the shock wave. When the shock reaches the zone with densities around  $10^{11} \text{ g cm}^{-3}$  in a few milliseconds after the bounce the  $\nu_e$ 's are released. This process is called neutronization burst. It has a peak luminosity of  $\sim 3.5 \times 10^{53} \text{ erg s}^{-1}$  and lasts  $\sim 25$  milliseconds. For a recent review of the current knowledge and status of the explosion mechanism, see [22].

At a distance  $d$  of the progenitor star, for each flavor  $\nu_\beta$  ( $\beta = e, \bar{e}, x$ ), the unoscillated spectral number fluxes ( $F_{\nu_\beta}^0(E)$ ) are:

$$F_{\nu_\beta}^0(E) = \frac{L_{\nu_\beta}}{4\pi d^2} \frac{f_{\nu_\beta}(E)}{\langle E_{\nu_\beta} \rangle}, \quad (1)$$

where  $L_{\nu_\beta}$  is the luminosity for the respective flavor  $\nu_\beta$ ,  $\langle E_{\nu_\beta} \rangle$  is the  $\nu_\beta$  mean energy and  $f_{\nu_\beta}(E)$  is the quasi-thermal spectrum written as follows [23]:

$$f_{\nu_\beta}(E) = \chi_\beta \left( \frac{E}{\langle E_{\nu_\beta} \rangle} \right)^{\alpha_\beta} e^{-(\alpha_\beta+1)E/\langle E_{\nu_\beta} \rangle}. \quad (2)$$

The  $\alpha_\beta$  is a parameter defined by  $\langle E_{\nu_\beta}^2 \rangle / \langle E_{\nu_\beta} \rangle^2 = (2 + \alpha_\beta) / (1 + \alpha_\beta)$  and  $\chi_\beta$  is the normalization constant factor:  $\int dE f_{\nu_\beta}(E) = 1$ . Several of these parameters, such as  $L_{\nu_\beta}$  in Eq. (1), and  $\langle E_{\nu_\beta}^2 \rangle$  and  $\langle E_{\nu_\beta} \rangle^2$  in Eq. (2), change their respective values with time after bounce and depend on the simulation of the star explosion [24].

After taking into account the effect of neutrino oscillations, in the three neutrino families framework in a supernova environment, the fluxes ( $F_{\nu_\beta}$ ) at Earth for each flavor  $\nu_\beta$  are [25]:

$$F_{\nu_e} = pF_{\nu_e}^0 + (1-p)F_{\nu_x}^0, \quad (3)$$

$$F_{\bar{\nu}_e} = \bar{p}F_{\bar{\nu}_e}^0 + (1-\bar{p})F_{\nu_x}^0 \quad (4)$$

and

$$4F_{\nu_x} = (1-p)F_{\nu_e}^0 + (1-\bar{p})F_{\bar{\nu}_e}^0 + (2+p+\bar{p})F_{\nu_x}^0, \quad (5)$$

where  $F_{\nu_\beta}^0$  are the primary unoscillated neutrino fluxes at the production region,  $x = \mu$  or  $\tau$  and  $p(\bar{p})$  is the survival probability of an electron (anti)neutrino after propagation through the SN mantle and the interstellar medium. For the actual oscillated parameters,  $p = 0$  for normal hierarchy (NH) ( $m_1 < m_2 \ll m_3$ ) and  $p = \sin^2 \theta_{12}$  for inverted hierarchy (IH) ( $m_3 \ll m_2 < m_1$ ).

For massive neutrinos, the arrival time ( $t_\oplus$ ) of the neutrino in the detector at Earth will be delayed [7]:

$$t_\oplus = t_i + d/c + \Delta t, \quad (6)$$

where  $t_i$  is the emission time at the source and  $c$  is the speed of light. The delay introduced by the neutrino mass  $m_\nu$  in Eq. (6) is represented by  $\Delta t$  and can be written as:

$$\Delta t = \frac{d}{2c} \left( \frac{m_\nu}{E} \right)^2. \quad (7)$$

## III. DETECTION ASSUMPTIONS

The neutrino flux of the neutronization burst is mainly populated by electronic neutrinos. Therefore, only experimental techniques with high sensitivity to  $\nu_e$  can have a possibility to investigate this particular phase of supernova explosion.

The Liquid Argon Time Projection Chamber (LArTPC), such as the ICARUS-like detectors [26], have all the features required to identify the neutronization burst. The “Long Baseline Neutrino Experiment” (LBNE) [27] foresees a 34 kton (fiducial volume) LArTPC as its far detector. The experiment is dedicated for determination of CP violation phase and neutrino mass hierarchy. Though, its dimensions and underground site are suitable for exploring rare events, such as neutrinos from supernovae and proton decay. This experimental design is taken into account for our calculations.

The most favourable electronic neutrinos ( $\nu_e$ ) detection channel in LArTPCs is the charged current (CC) interaction:  $\nu_e + {}^{40}\text{Ar} \rightarrow e^- + {}^{40}\text{K}^*$ . There are other detection channels, but all of them with smaller cross section. These detection channels can be tagged by spectral analysis of the photon emission from de-excitation of  $K$ ,  $Cl$  or  $Ar$ , which exhibit specific spectral lines. The  $\nu - Ar$  cross sections can be found in Fig. 3 of Ref. [28].

#### IV. CALCULATION METHOD

The number of expected events in the detector can be evaluated in the following way:

$$\frac{dN}{dt}(t_{\oplus}) = \frac{n_t}{4\pi d^2} \int dE \sigma(E) \int dt_i F_{\nu_{\beta}}(E, t_i) \delta(t_{\oplus} - t_i - \Delta t), \quad (8)$$

where  $\sigma(E)$  is the  $\nu_e - Ar$  CC cross section,  $n_t$  is the number of targets in the 34 kton Argon detector and  $F_{\nu_{\beta}}(E, t_i)$  is the oscillated neutrino flux, which is evaluated by Eqs. (1-5).

We performed a Monte Carlo simulation (MC) with very optimistic assumptions. Nevertheless, all of our assumptions have solid grounds and can be taken as a “realistic case”. The number of expected events depends on the considerations we make about the neutrino production and their propagation till the detector. We considered a comprehensive knowledge of the astrophysical process related to the SN explosion, which means that the astrophysical parameters related to neutrino production, ie the neutrino fluxes, are well known. However, to introduce uncertainties related to the explosion mechanism, we considered a 5% error in the overall normalization of the evaluated counting rates. Concerning the SN distance, we assumed a galactic SN of 10 kpc. The detector configuration, as pointed out before, is 34 kton LArTPC with 80% of efficiency for  $\nu_e$  charged current (CC) detection. For now, background effects have been disconsidered since the detector is assumed to be placed underground. In this situation we expect a suppression of seven orders of magnitude [29]. The  $\nu_e$  energy threshold for detection was set to 5 MeV. For the energy resolution we used a parametrization given by:  $11\%/\sqrt{E(\text{MeV})} + 2\%$  [30]. For the time resolution, we adopted a  $\pm 20 \mu\text{s}$  flat distribution. Also, we stress the fact that we performed our MC ignoring additional complications given by the lack of knowledge if the first detected event is synchronized or not with the beginning of the burst. In the MC we included the two possible scenarios for mass hierarchy, as mentioned in Sec. II, with the best-fit values of the oscillation parameters with no CP violation effects [31].

#### V. RESULTS

Our MC simulation results in thinner lines are shown in Fig. 1. NH and IH hierarchy are represented by solid and dashed lines, respectively. The error bars in each bin are assumed to follow a Poissonian distribution and each bin has  $\delta t = 0.005$  s width. In Fig. 1, we also show the expected number of events in the thicker lines considering a 0.5 eV neutrino mass, just for comparison with our MC.

Non vanishing neutrino mass causes a delay in the experimental signal, changing the expected number of events in each time bin, as we can notice analysing Eq. (7) and Eq. (8). These theoretical modifications can be compared with the number of events in each bin generated by our MC simulation using the  $\chi^2$  test:

$$\chi^2 = \sum_{i=1}^N \frac{(N_i^{MC} - N_i(m_{\nu}))^2}{\sigma_i^2}, \quad (9)$$

where  $i = 1, N$  bins,  $N_i^{MC}$  is the number of events generated by our MC in the  $i$ -bin,  $N_i(m_{\nu})$  is the number of events evaluated by Eq. (7) and Eq. (8) for different neutrino masses ( $m_{\nu}$ ) and  $\sigma_i$  is the associated error.

The “realistic case” provided  $\chi_{min}^2 \approx 2.12$  for a neutrino mass of  $m_{\nu} = 0.00$  eV and considering NH. From the  $\Delta\chi^2 = \chi^2(m_{\nu}) - \chi_{min}^2$ , the upper bound on neutrino mass from the  $\nu_e$  neutronization burst stage is, at 95% C.L, 2.71 eV. On the other hand, for the IH case, we have obtained  $\chi_{min}^2 \sim 5.43$  for a neutrino mass of  $m_{\nu} \approx 1.00$  eV. At 95% C.L,  $0.18 \text{ eV} \lesssim m_{\nu} \lesssim 1.70 \text{ eV}$ . We present our  $\Delta\chi^2$  in terms of the neutrinos mass,  $m_{\nu}(\text{eV})$ , in Fig. 2, for both

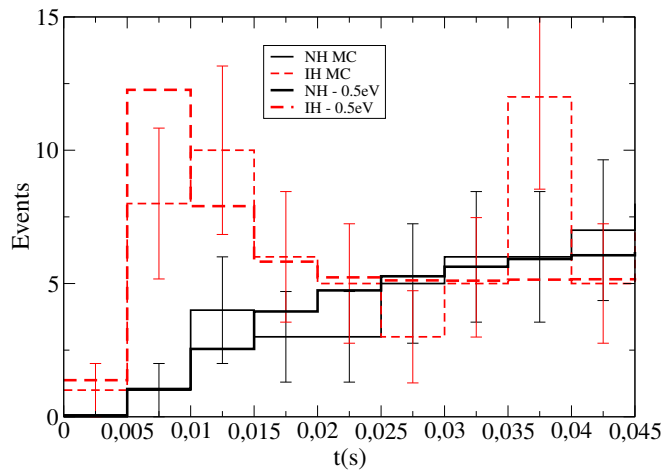


FIG. 1: (*Colours online*) Results of our Monte Carlo realization. For further details see text. Normal hierarchy (NH) in solid curves and inverted hierarchy (IH) in dashed curves. Thicker lines represent the expected number of events for a 0.5 eV neutrino mass.

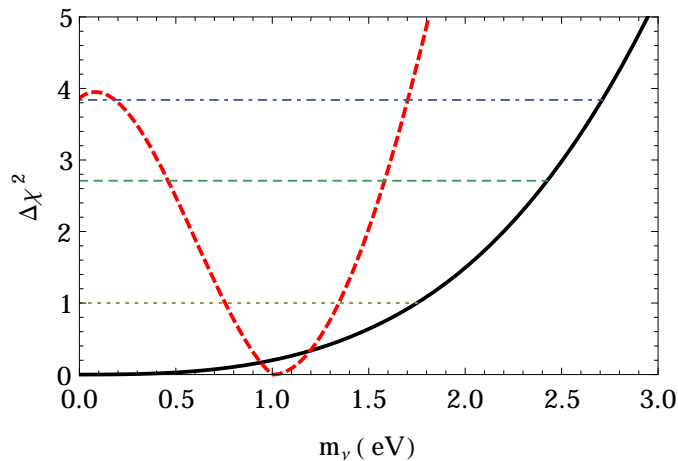


FIG. 2: (*Colours online*) Neutrino mass bound considering a supernova at 10 kpc and a liquid argon detector with 34 kton, such as the one projected in the LBNE experiment. Dotted line is  $1\sigma$  limit; dashed line is the  $2\sigma$  limit; and dotted-dashed line is the  $3\sigma$  limit. The strong red dashed curve is for IH and the strong solid black curve is for NH.

hierarchies. In these plots, dotted lines are bounds with 68.27% C.L, dashed lines are for 90% C.L; and dotted-dashed lines are the 95% C.L.

We also performed other MC simulations and did the  $\chi^2$  analysis for the mass as a parameter for other situations that are described in the following:

1. “perfect case”: we consider that the normalization is completely known, 100% of detector efficiency and a perfect time and energy resolution. We maintain an energy cutoff in 5 MeV;
2. “perfect norm”: returning to the conditions established in “realistic case”, but now for a completely known supernova normalization;
3. “perfect eff”: considering a detector with 100% of efficiency and other conditions of the “realistic case” maintained;
4. “cut ener”: keeping the “realistic case”, but instead cutting events with energy less than 5 MeV, we perform a energy cut at  $\approx 2.2$  MeV;
5. “time resol”: considering a temporal resolution of 1 ms instead of 20  $\mu s$  of the “realistic case”;
6. “bin1”: if we increase the bin size from 5 ms to 10 ms using the “realistic case” and

7. “bin2”: if we decrease the bin size from 5 ms to 2 ms using the other conditions of the “realistic case”

We present in Table I our mass boundaries at 68.27%, 90% and 95% C.L for NH. The numbers in parentheses are the boundaries for IH. In this table we also show the minimum value of the mass ( $m_{min}$ ) with its respective  $\chi^2$ , the  $\chi_{min}^2$ .

|              | 68.27% C.L      | 90% C.L         | 95% C.L         | $m_{min}$   | $\chi_{min}^2$ |
|--------------|-----------------|-----------------|-----------------|-------------|----------------|
| realistic    | 1.75(0.76-1.35) | 2.43(0.46-1.58) | 2.71(0.18-1.70) | 0.00 (1.00) | 2.12 (5.43)    |
| perfect norm | 0.91-3.25(0.65) | 3.79(0.95)      | 4.07(1.1)       | 2.27 (0.00) | 8.51 (3.22)    |
| perfect eff  | 2.01(0.82)      | 2.52(1.08)      | 2.76(1.20)      | 1.10 (0.00) | 2.39 (3.06)    |
| cut ener     | 2.05(0.69)      | 2.58(1.03)      | 2.87(1.20)      | 1.22 (0.00) | 7.53 (6.34)    |
| time resol   | 1.34(0.71)      | 1.94(1.03)      | 2.22(1.17)      | 0.00 (0.00) | 2.33 (8.53)    |
| bin1         | 0.71-2.23(0.63) | 2.66(0.93)      | 2.88(1.09)      | 1.54 (0.00) | 0.51 (3.22)    |
| bin2         | 1.65(2.24-2.67) | 2.14(2.03-2.91) | 2.38(1.90-3.06) | 0.81 (2.50) | 4.84 (9.74)    |
| perfect      | 3.26(0.96)      | 3.74(1.19)      | 3.96(1.29)      | 2.37 (0.50) | 12.20 (4.41)   |

TABLE I: Upper Bounds on  $m_\nu$ (eV) considering a supernova at 10 kpc and a liquid argon detector with 34 kton. We show the results for normal hierarchy (NH) and the numbers inside the parentheses are the mass evaluation for inverted hierarchy (IH). Also we show the the minimum value of the mass ( $m_{min}$ ) with its respective  $\chi^2$ , the  $\chi_{min}^2$ . For details of the meaning of each test, see the text.

## VI. DISCUSSION

From Table I we notice that, despite we change the configuration of the detector, statistical fluctuation of the Monte Carlo simulation plays a fundamental role in the mass bound determination, since we have few events in the neutronization burst and this process lasts only  $\approx 25$  ms. A very good example of this kind of behaviour is the one shown in the IH curve of Fig. 1 (red dashed). In the interval of 35-40 ms, there is a peak that was not theoretically predicted. So, this generates a worse  $\chi^2$  and an interval in the neutrino mass bound (0.18-1.70 eV) with a  $\chi_{min}^2$  at 1.00 eV. Another example of the impact of this statistical fluctuation is that, for the NH case, we have obtained a more stringent bound in the “realistic” case compared to the “perfect” case.

Our bound, at 95% C.L, for the NH is very similar to the one obtained by the Troitsk experiment of tritium  $\beta$  decay. So, if we really have NH and comparing with terrestrial experiments, which are independent of mass hierarchy, like Katrin ( $m_\nu < 0.2$  eV), it will be very difficult that LBNE will put a more stringent limit on neutrino mass. From the Planck Cosmic Microwave Background measurements and galaxy clustering information from the Baryon Oscillation Spectroscopic Survey (BOSS), part of the Sloan Digital Sky Survey-III, and assuming a  $\Lambda$ CDM cosmological model, Ref. [32] obtained, at 95% C.L,  $\sum m_\nu < 0.35$  eV. Ref. [33] obtained that  $\sum m_\nu < 0.18$  eV, when one takes into account observations of the large-scale matter power spectrum from the WiggleZ Dark Energy Survey, Planck satellite and baryon acoustic oscillation. If we consider that mass eigenstates are degenerated,  $m_\nu \lesssim 0.12$  eV [32] and  $m_\nu \lesssim 0.06$  eV [33].

For the NH and IH case, our bounds, respectively, at 95% C.L, are  $m_\nu < 2.71$  eV and  $0.18$  eV  $< m_\nu < 1.70$  eV. These bounds are almost similar with other prospects of neutrino mass bounds obtained for SN neutrinos. Just for comparison, authors in [34] considering only normal hierarchy, using a 20 kton liquid scintillator at Jiangmen Underground Neutrino Observatory (JUNO) and a galactic supernova  $\bar{\nu}_e$  signal obtained a limit on the absolute neutrino mass scale:  $m_\nu < (0.83 \pm 0.24)$  eV at 95% C.L. This limit is also similar with the ones obtained in the other cases discussed in this work - see Table I. So, our conclusion here is that, for a SN at 10 kpc of distance and  $15 M_\odot$ , LBNE 34 kton argon detector can probe neutrino masses of order of 1 eV, at 95% C.L. We stress the fact that knowing neutrino mass hierarchy is fundamental to put limits on neutrino masses from SN and LBNE has as one of its objectives determine this property.

## VII. CONCLUSIONS

Even though our supernova neutrino bound seems not to be competitive with the prospective Katrin bound, the neutrino mass bound from SN has a lot merit and importance, and, of course, it should be a source of strong investigation. With improvements in the detector efficiency, the number of events per bin would increase and a more

competitive bound could be obtained. We remember that efficiency includes several effects, such as, loss of events due to light attenuation, fluctuations of the number of photoelectrons, the geometry of the detector etc. These are still unknown sources of errors, and their knowledge is crucial for a more detailed work than presented here. We are aware that our assumptions are very crude, however, as stated by the LBNE collaboration in [27], work in understanding the physics and choices of detector is still underway. It is necessary to determine, for example, the low energy response of the detector, its geometry, its real threshold, the reconstruction of the events, event vertex resolution, the energy resolution, absolute event  $ms$  time precision and other details. That is why we are being very conservative, but at the same time, very optimistic in this work. However, we should stress that considering this time binned analysis, we have demonstrated that statistical fluctuation may play a major role in the determination of the neutrino mass bound. We point out that a more dedicated MC simulation, with real and proper detector information, with an effective study of a possible event-by-event likelihood of detection for this flux of  $\nu_e$  of neutronization burst and, finally, the importance of the time of the first event detected should be studied deeply in the foreseeable future.

### Acknowledgments

F. Rossi-Torres would like to thank CNPq for the full financial support. E. Kemp would like to thank FAPESP and CNPq for partial financial support. M. M. Guzzo also would like to thank CNPq for partial financial support to this work. Also, we would like to thank prof. H.-T. Janka for providing the data of supernova simulation used to calculate neutrino fluxes.

- 
- [1] Q. R. Ahmad *et al.* [SNO collaboration], Phys. Rev. Lett. **89** (2002) 011301.
  - [2] K. Eguchi *et al.* [KamLAND Collaboration], Phys. Rev. Lett. **90** (2003) 021802.
  - [3] M. Steidl, arXiv:0906.0454 [nucl-ex].
  - [4] J. Beringer *et al.* [Particle Data Group Collaboration], Phys. Rev. D **86**, 010001 (2012).
  - [5] V. N. Aseev *et al.* [Troitsk Collaboration], Phys. Rev. D **84**, 112003 (2011) [arXiv:1108.5034 [hep-ex]].
  - [6] R. G. H. Robertson [KATRIN Collaboration], arXiv:1307.5486 [physics.ins-det].
  - [7] G.T. Zatsepin, Pisma Zh. Eksp. Teor. Fiz. **8** (1968) 333.
  - [8] K.S. Hirata *et al.*, Phys. Rev. D **38** (1988) 448; K. Hirata *et al.* [Kamiokande-II Collaboration], Phys. Rev. Lett. **58** (1987) 1490.
  - [9] R.M. Bionta *et al.*, Phys. Rev. Lett. **58** (1987) 1494; C.B. Bratton *et al.* [IMB Collaboration], Phys. Rev. D **37** (1988) 3361.
  - [10] E.N. Alekseev, L.N. Alekseeva, V.I. Volchenko and I.V. Krivosheina, JETP Lett. **45** (1987) 589; E.N. Alekseev, L.N. Alekseeva, I.V. Krivosheina and V.I. Volchenko, Phys. Lett. B **205** (1988) 209.
  - [11] A. Ianni, G. Pagliaroli, A. Strumia, F. R. Torres, F. L. Villante and F. Vissani, Phys. Rev. D **80**, 043007 (2009) [arXiv:0907.1891 [hep-ph]].
  - [12] G. Pagliaroli, F. Rossi-Torres and F. Vissani, Astropart. Phys. **33**, 287 (2010) [arXiv:1002.3349 [hep-ph]].
  - [13] T.J. Loredo and D.Q. Lamb, Phys. Rev. D **65** (2002) 063002.
  - [14] E. Nardi and J.I. Zuluaga, Phys. Rev. D **69** (2004) 103002.
  - [15] E. Nardi and J.I. Zuluaga, Nucl. Phys. B **731** (2005) 140.
  - [16] J.I. Zuluaga, PhD thesis defended on 2005 at the Univ. de Antioquia, Medellin, astro-ph/0511771v2.
  - [17] J. Ellis, H. -T. Janka, N. E. Mavromatos, A. S. Sakharov and E. K. G. Sarkisyan, Phys. Rev. D **85**, 105028 (2012) [arXiv:1202.0248 [hep-ph]].
  - [18] F. Vissani, G. Pagliaroli and F. Rossi-Torres, Int. J. Mod. Phys. D **20**, 1873 (2011).
  - [19] R. Laha, J. F. Beacom and S. K. Agarwalla, arXiv:1412.8425 [hep-ph].
  - [20] C. Lujan-Peschard, G. Pagliaroli and F. Vissani, JCAP **1407**, 051 (2014) [arXiv:1402.6953 [astro-ph.SR]].
  - [21] R. Laha and J. F. Beacom, Phys. Rev. D **89**, no. 6, 063007 (2014) [arXiv:1311.6407 [astro-ph.HE]].
  - [22] H. -T. Janka, F. Hanke, L. Huedepohl, A. Marek, B. Mueller and M. Obergaulinger, PTEP **2012**, 01A309 (2012) [arXiv:1211.1378 [astro-ph.SR]].
  - [23] M. T. Keil, G. G. Raffelt and H. -T. Janka, Astrophys. J. **590**, 971 (2003) [astro-ph/0208035].
  - [24] M. Kachelriess, R. Tomas, R. Buras, H. -T. Janka, A. Marek and M. Rampp, Phys. Rev. D **71**, 063003 (2005) [astro-ph/0412082].
  - [25] A. S. Dighe and A. Y. Smirnov, Phys. Rev. D **62**, 033007 (2000) [hep-ph/9907423].
  - [26] C. Rubbia, 1977, CERN-EP-INT-77-08.
  - [27] C. Adams *et al.* [LBNE Collaboration], arXiv:1307.7335 [hep-ex]; <http://lbne.fnal.gov/>
  - [28] I. Gil Botella and A. Rubbia, JCAP **0310**, 009 (2003) [hep-ph/0307244].
  - [29] V. Gehman, Private Communication (2014).
  - [30] S. Amoruso *et al.* [ICARUS Collaboration], Eur. Phys. J. C **33**, 233 (2004) [hep-ex/0311040].

- [31] D. V. Forero, M. Tortola and J. W. F. Valle, Phys. Rev. D **86**, 073012 (2012) [arXiv:1205.4018 [hep-ph]].
- [32] Elena Giusarma, Roland de Putter, Shirley Ho, Olga Mena, Phys.Rev. **D88**, 063515 (2013), arXiv:1306.5544 [astro-ph].
- [33] S. Riemer-Sørensen, D. Parkinson and T. M. Davis, Phys. Rev. D **89**, no. 10, 103505 (2014) [arXiv:1306.4153 [astro-ph.CO]].
- [34] J. S. Lu, J. Cao, Y. F. Li and S. Zhou, arXiv:1412.7418 [hep-ph].